Journal of Molecular Structure 1269 (2022) 133779

Contents lists available at ScienceDirect

Journal of Molecular Structure

journal homepage: www.elsevier.com/locate/molstr

Synthesis, structural characterization and X-ray analysis of (E)-N'-((2-hydroxynaphthalen-1-yl)methylene)-4-ethylbenzenesulfonohydrazide and Its Ni(II) complex

Murat Çınarlı*

Central Research and Application Laboratory, Kırşehir Ahi Evran University, Central Research and Application Laboratory, 40100 Kırşehir, Turkey

ARTICLE INFO

Article history:
Received 8 June 2022
Revised 11 July 2022
Accepted 21 July 2022
Available online 23 July 2022

Keywords:
Sulfonohydrazone
X-ray single crystal
2-benzoyl pyridine
Metal complexes of sulfonylhydrazone
Antimicrobial activities

ABSTRACT

A new p-toluene sulfonyl hydrazide derivative sulfonyl hydrazone and its Ni(II) complex have been synthesized. The ligand (E)-N'-((2-hydroxynaphthalen-1-yl)methylene)-4-ethylbenzenesulfonohydrazide (HL) was characterized by using elemental analysis, FT-IR, ^{1}H-NMR, UV-Vis., LC/MS and X-ray single crystal methods. The structure of Ni(II) complex (1) investigated using elemental analysis, FTIR, UV-Vis., LC/MS and magnetic suscebtibility studies. The ligand (HL) crystallized in the monoclinic structure and the P $2_1/c$ space group. All data reveal that the Ni(II) complex [NiL_2] possesses 1:2 metal-ligand ratio. A square planar structure is proposed for the Ni(II) complex on the basis electronic spectrum and magnetic evidence. Ligand coordination take place through the azomethine nitrogen and the sulfonyl oxygen atom. Additionally, the ligand and its complex were examined for their antimicrobial activity against pathogenic microorganisms using the minimal inhibitory concentration method (MIC). It was found that the inhibitory effects of the [NiL_2] and the ligand were similar.

1. Introduction

The biggest challenges for treating diseases are the ability of pathogens to develop drug resistance, the lack of antibiotics to kill bacteria, and the emergence of new pathogens. Therefore, studies on the development of new antibacterial agents are critical.

Sulfa drugs, which were developed in the 1930s, were the first important compounds to treat bacterial infections. The invention of this compound triggered the discovery of other antibacterial sulfonamides and sulfonyl hydrazone derivatives [1,2]. Sulfonyl hydrazone and sulfonyl hydrazide derivatives exhibit a wide spectrum of biological properties such as antibacterial, antitumor, anti-carbonic anhydrase, diuretic, hypoglycemic, anti-thyroid, protease inhibitor and anticonvulsant activities [3–10]. Sulfonylhydrazone compounds containing different donor atoms have an important place in coordination chemistry. Nevertheless, compounds containing both a Schiff base and sulfonamide fragments are known to compounds with significant antibacterial properties.

In our previous studies, we synthesized new sulfonyl hydrazones and their metal complexes and tested them for antibacterial activity [11,12]. In this work, new sulfonylhydrazone ligand (E)-N'-((2-hydroxynaphthalen-1-yl)methylene)-4-ethylbenzenesulfonohydrazide **(HL)** and its Ni(II) complex (1) were synthesized. The structure of **HL** has been investigated using elemental analysis, FT-IR and UV-Vis. spectrophotometric methods. The structure of HL was confirmed by ^{1}H NMR. The structure of **HL** has been investigated by X-ray diffraction method. The structure of Ni(II) complex (1) investigated using elemental analysis, FTIR, UV-Vis., LC/MS and magnetic suscebtibility studies. The ligand and its Ni(II) complex were screened for antibacterial activity against clinically important human pathogens using the minimal inhibitory concentration method (MIC).

2. Experimental

2.1. Materials

All materials used in this investigation were purchased from Sigma/Aldrich. All chemicals purchased from commercial suppliers were of reagent grade and were used without further purification.

2.2. Physical measurements

The elemental analysis was performed on a Thermo Flash 2000 Elemental Analyser. The electronic absorption spectra of the title compounds were recorded at room temperature in DMSO solution

* Corresponding author at: Kırşehir Ahi Evran University, Central Research and Application Laboratory, 40100 Kırşehir, Turkey.
E-mail address: murat.cinarli@ahievran.edu.tr

https://doi.org/10.1016/j.molstruc.2022.133779
0022-2860/

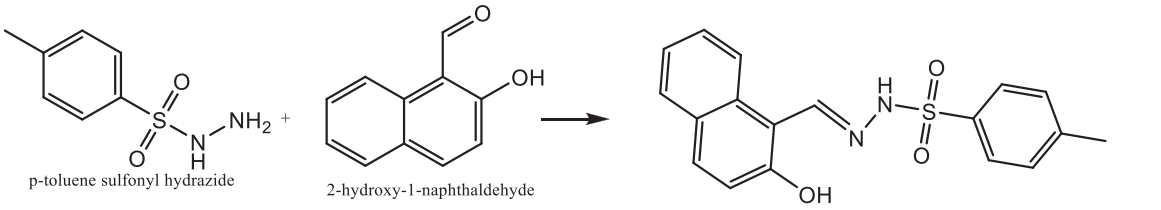

(*E*)-*N*'-((2-hydroxynaphthalen-1-yl)methylene)-4-methylbenzenesulfonohydrazide

Scheme 1. Synthesis of HL.

on a Thermo Evolution UV-Visible spectrophotometer working between 200-1100 nm. IR spectra were recorded on Thermo Scientific Nicolet iS10 FT-IR spectrophotometer using ATR. ^{1}H NMR spectra were measured in DMSO-*d*6 on a Agilent 600 MHz NMR spectrophotometer.

2.3. X-ray crystallography

The data collection was performed at 296 K on a Bruker APEX-II CCD image plate detector using a graphite monochromated Mo-Kα radiation (λ = 0.71073 Å). The structure was solved by direct methods using SHELXS [13] implemented in the WinGX software system [14] and refined using full-matrix least-squares procedure on F^2 using SHELXL [15]. The hydrogen atoms of the compound are obtained refining isotropic while other atoms are refined anisotropically. The parameters of some groups are found at CH = 0.93 Å (for phenyl ring and methine), CH_3 = 0.96 Å, NH = 0.86 Å and OH = 0.82 Å Uiso(H) = 1.2Ueq (1.5 for OH and methyl groups).

2.4. Preparations

2.4.1. Synthesis of the HL

A solution of p-toluene sulfonyl hydrazide (0.186 g, 1 mmol) in ethanol (20 mL) was added dropwise to a hot ethanolic solution (20 mL) of the 2-hydroxy-1-naphthaldehyde (0.172 g, 1 mmol). The reaction mixture was refluxed with stirring for 6 h and kept at room temperature for slow evaporation. The pale yellow crystalline compound was filtered and recrystallized with ethanol. Yield: 82%, Mp.: 166°C. Elemental Anal. Found (Calcd.) (%): C: 62.81 (63.51), H: 4.73 (4.74), N: 7.33 (8.23), S: 9.87 (9.42). LC-MS of [M^+], m/z Calc. for $C_{18}H_{16}N_2O_3S$ 340.39; found 340.80 (S1). The chemical structure of **HL** is shown in Scheme 1.

2.4.2. Synthesis of [NiL_2]

A solution of $Ni(CH_3COO)_2.4H_2O$ (0.0496 g, 0.2 mmol) in ethanol (10 mL) was added to a hot solution containing **HL** (0.136 g, 0.4 mmol) in ethanol (20 mL). The reaction mixture was refluxed for 2–3 h and then left to cool. The greenly solid complexes formed were collected by filtration and dried in a desiccator. Although different solvents and different experimental methods were tried for the Ni(II) complex, the suitable crystal for single-crystal X-ray diffraction methods could not be obtained. Yield: 72%, Mp(decomp.): 322 °C. Elemental Anal. Found (Calcd.) (%): C: 59.42 (58.47), H: 4.18 (4.36), N: 7.90 (7.58). LC-MS of [NiL_2]$^+$, m/z Calc. for $C_{36}H_{30}N_4O_6S_2Ni$ 737.47; found 738.67 (S2). The chemical structure of **1** is shown in Scheme 2.

2.4.3. Detection of antibacterial activity

The well diffusion method was used to evaluate the antimicrobial activity of the nickel complex and its ligand on clinically important human pathogens. *B. cereus* CU1065, *B. subtilus* ATCC 6633, *E. coli* ATCC 25922, *E. faecalis* ATCC 29212, *K. pneumoniae* ATCC 13883, *P. aeruginosa* ATCC 27853 and *S. aureus* ATCC 29213 strains were used as indicator strains in the study. The strains used were obtained from Kırşehir Ahi Evran University, Faculty of Arts and Sciences, Microbiology Laboratory. In this study, Tryptone Soy Broth medium (TSB) was used for developing of type strains. Cultures were diluted to 1 × 10^6 CFU/mL after 1 night incubation at 37°C. The nickel complex and ligand were dissolved in dimethyl sulfoxide (DMSO) to a final concentration of 200 µg/mL.

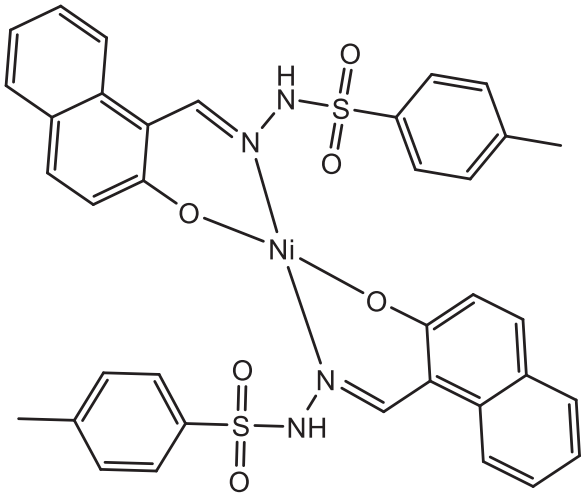

Scheme 2. Synthesis of [NiL_2] complex.

After the cultures with a final concentration of 1 × 10^6 CFU/mL were spread homogeneously on Mueller Hinton Agar (Merck) media with a sterile drigalski spatula, 6 mm diameter wells were opened on their plates. 100 µL of Ni complex and 100 µL of ligand solution were added to the opened wells and left for 2 h at room temperature. After 24 h of incubation at 37°C, antimicrobial activity results were evaluated by measuring the zone diameter around the wells in mm and averaging the three runs.

3. Results and discussion

3.1. Structure description of the HL

The organic compound the closed formula $C_{18}H_{16}N_2O_3S$ includes azomethine (C=N), sulfano, and naphthalene groups. The organic compound crystallized in the monoclinic structure and the P 2_1/c space group. Ortep-3 [16] drawing of the title compound **(HL)** in the asymmetric unit is shown in Fig. 1. Some important data parameters on this molecular structure are given in Table 1. Also, some selected bond parameters of the molecular structure are given in Table 2. When some bond parameters of the molecular structure were compared with similar studies in the literature,

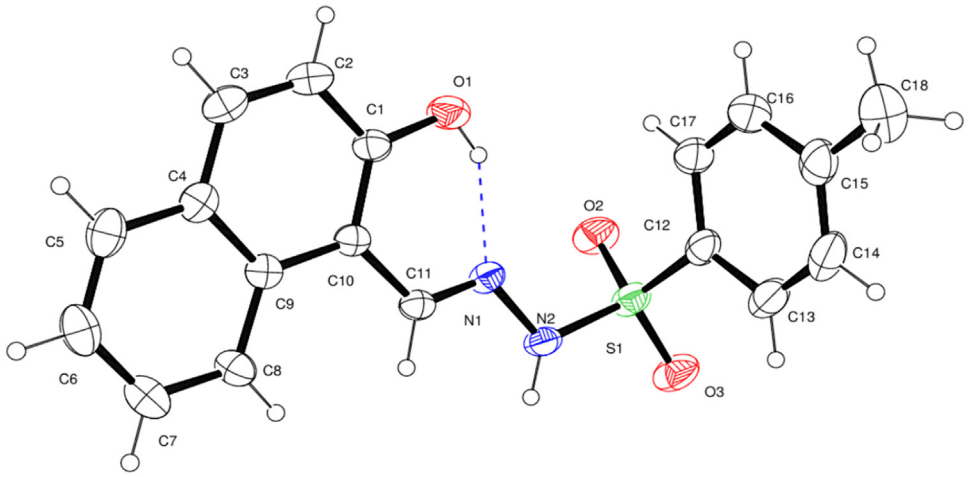

Fig. 1. ORTEP-3 drawing of the molecular structure (HL) with the atom-numbering scheme. Displacement ellipsoids are drawn at the 30% probability level.

Table 1
Crystallographic data of HL.

Empirical formula	$C_{18}H_{16}N_2O_3S$
Molecular weight	340.39
Temperature, T (K)	296
Wavelength (Å)	0.71073
Crystal system	Monoclinic
Crystal size (mm^3)	0.011 × 0.012 × 0.013
Space group	P $2_1/c$
a (Å)	15.7709(5)
b (Å)	10.5572(4)
c (Å)	10.3234(3)
α (°)	90
β (°)	104.1180(10)
γ (°)	90
Volume, V ($Å^3$)	1666.89(10)
Z	4
Calculated density (Mg m^{-3})	1.356
θ Range (°)	2.34 – 22.05
Index ranges	h=-18→18, k=-12→12, l=-12→12
Measured reflections	27520
Independent reflections	2934
Observed reflections (I>2σ)	1998
Goodness-of-fit on F^2	1.133
R1 indice (I>2σ)	0.0477
wR2 indice (I>2σ)	0.121
$\Delta\rho_{min}$, $\Delta\rho_{max}$ (e/$Å^3$)	-0.295, 0.381
R_{int}, R_{sigma}	0.0581, 0.0377
CCDC number	2143082

Table 2
Selected geometrical parameters of HL.

	X-ray results		X-ray results
Bond lengths (Å)		Torsion angles (°)	
N(1)–N(2)	1.399(3)	N(1)–N(2)–S(1)–C(12)	62.0(2)
N(1)–C(11)	1.280(3)	N(1)–N(2)–S(1)–O(2)	-53.8(2)
N(2)–S(1)	1.644(2)	N(1)–N(2)–S(1)–O(3)	178.1(2)
O(1)–C(1)	1.355(3)	C(11)–N(1)–N(2)–S(1)	-173.3(2)
S(1)–O(2)	1.430(2)	C(10)–C(11)–N(1)–N(2)	179.7(2)
S(1)–O(3)	1.427(2)	O(1)–C(1)–C(10)–C(11)	2.2(4)
S(1)–C(12)	1.758(3)		
Bond angles (°)			
N(1)–N(2)–S(1)	113.5(2)	N(2)–S(1)–O(3)	104.0(2)
N(2)–N(1)–C(11)	117.9(2)	O(2)–S(1)–C(12)	108.4(2)
N(1)–C(11)–C(10)	121.1(2)	O(3)–S(1)–C(12)	109.8(2)
N(2)–S(1)–C(12)	106.8(2)	O(2)–S(1)–O(3)	120.3(2)
N(2)–S(1)–O(2)	106.5(2)		

Table 3
Hydrogen bond interactions of HL (Å, °).

Hydrogen bond(Å,°)	D–H	H...A	D...A	D–H...A
O(1)–H(1)...N(1)	0.82	1.84	2.567(3)	146
N(2)–H(2A)...O(2)^{i}	0.86	2.36	3.000(3)	131
C(14)–H(14)...O(3)^{ii}	0.93	2.52	3.424(4)	165

Symmetry codes: (i) x,1/2-y,1/2+z; (ii) -x,-1/2+y,1/2-z.

it was observed that the bond lengths were quite compatible. In the hydrazone group (CH = N – NH) of the molecular structure, we can say that N(1)–C(11) (1.280(3) Å) bond length is similar to the literature results [17, 18] (N(1)–C(7) (1.272 (4)Å)) and this bond is double bond character.

The bond lengths of these bonds and N(1)–N(2) and O(1)–C(1) bonds are quite consistent with the values in the literature [12, 19–21]. The dihedral angle of the hydrazone group (C(11)=N(1)–N(2)) is 117.9(2)°. This result is in good agreement with the related literature [17].

In order to investigate the aromaticity of rings, (HOMA) indices for rings by using following equation:

$$HOMA = 1 - \left[\frac{\alpha}{n}\sum_{i=1}^{n}(R_i - R_{opt})^2\right] \quad (1)$$

In Eq. (1), n is the number of bonds in a ring, α is the constant equal to 257.7 and R_{opt} is equal to 1.388 Å for C–C bonds. The HOMA (harmonic oscillator model of aromaticity) value allows us to decide whether a compound is completely aromatic. If its value is 1, the compound is aromatic and if 0, the compound is not aromatic [21, 23]. The HOMA values for C(12)–C(17) phenyl and C(1)–C(10) naphthalene rings are 0.9698 and 0.7948, respectively. According to the results, we can say that these rings are an aromatic ring structure.

The molecular structure has an intra and two intermolecular O–H…N and C/N–H…O hydrogen bonds. The hydrogen bond values of the molecular structure are given in Table 3. As can be seen from Fig. 2a-2b and Table 3, due to the short H...A bond distances the intermolecular hydrogen bonds are highly effective in the single crystal packing. According to PLATON [22] drawing of its crystal packing, N(2)–H(2A)…O(2)^{i} [(i) x,1/2-y,1/2+z] intermolecular hydrogen bond of the compound forms the C(4) chain and continues along the $\mp c$ direction of the unit cell (see Fig. 2a). Also, C(14)–H(14)…O(3)^{ii} [(ii) -x,-1/2+y,1/2-z] intermolecular hydrogen bond of the compound forms the C(6) zigzag chain and continues along the $\mp b$ direction of the unit cell (Fig. 2b).

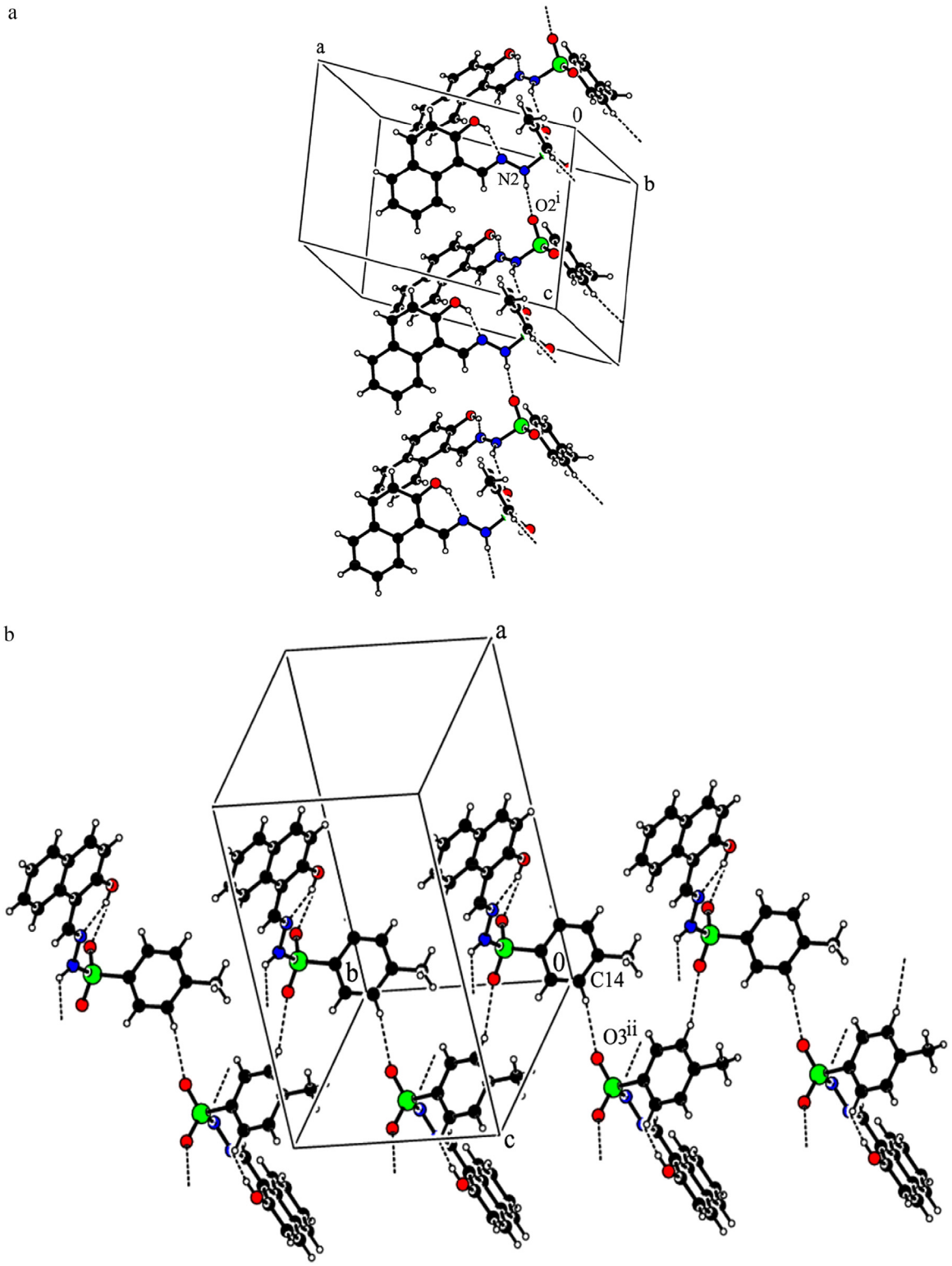

Fig. 2. a) PLATON drawing of HL formed polymeric chain with symmetry code. (i): x,1/2-y,1/2+z; b) PLATON drawing of HL formed zigzag chain with symmetry code. (ii): -x,-1/2+y,1/2-z

3.2. ^{1}H-NMR studies of (HL)

^{1}H NMR spectrum of the ligand (see Fig. 3) in DMSO-d^6 confirmed the proposed structure for **HL**. The OH proton of the ligand was observed at 11.52 ppm as a singlet. In ^{1}H NMR spectrum of **HL**, the singlet peak at 11.13 ppm was due to the N-H proton. The –CH=N– proton signaled at 8.80 ppm. The other values obtained for ^{1}H-NMR chemical shifts of the ligand were (CH_3) at 3.16 ppm and (Ar-H) at 7.08–8.34 ppm [1,24].

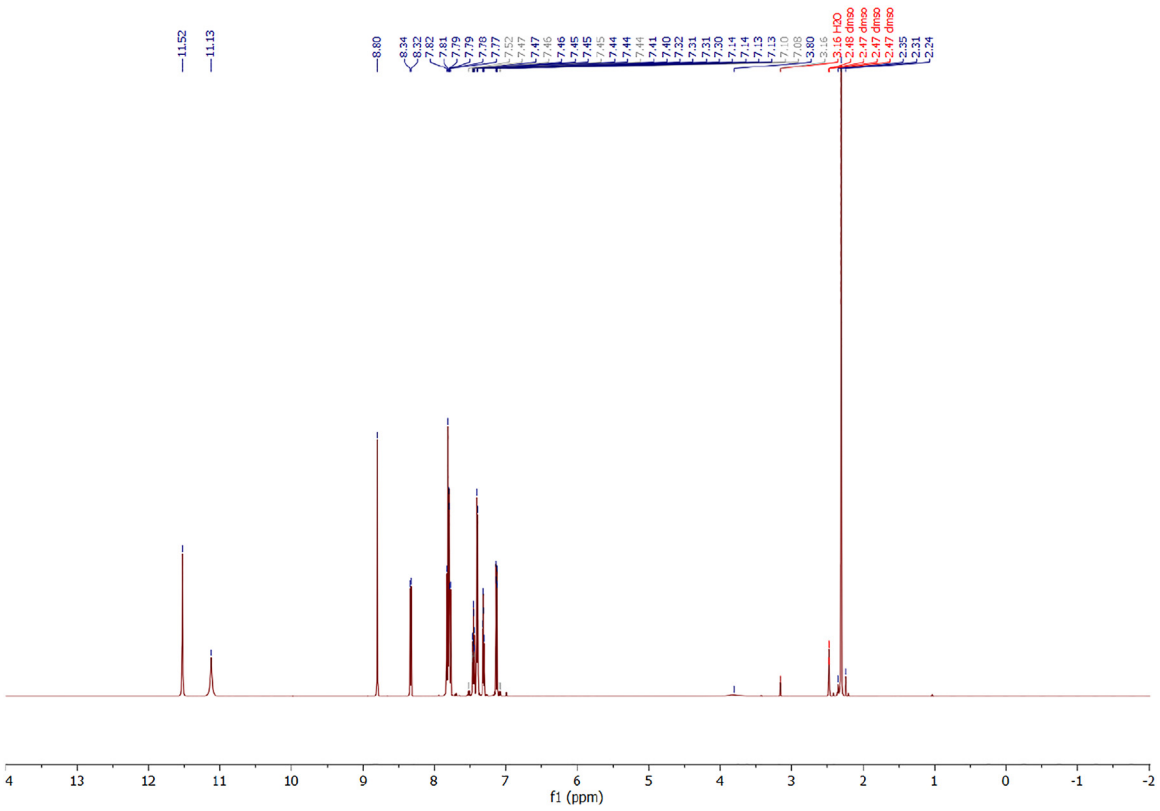

Fig. 3. ^{1}H NMR spectrum of the HL.

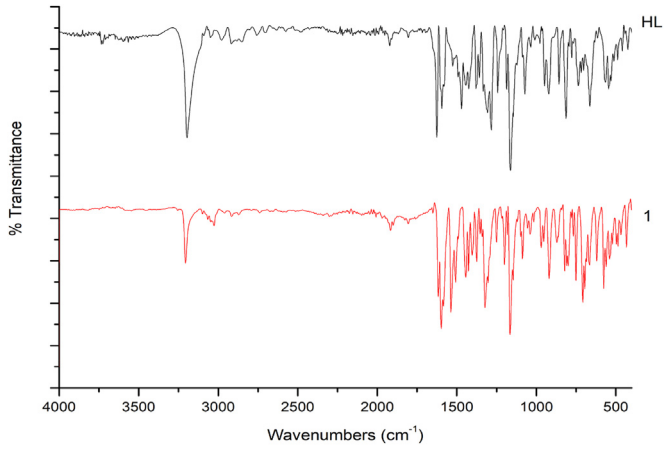

Fig. 4. IR spectra of HL and 1.

3.3. IR studies of the HL

Fig. 4 shows the assignment of the main bands in the FT-IR spectra of the free ligand and its Ni(II) complex, based on some general references and previous studies on sulfonamides or sulfonyl hydrazones.

The strong absorption band at 3196 cm^{-1} was assigned to the NH group, while the OH band appeared at around 3048 cm^{-1} next to the sharp NH band. The IR spectrum of the ligand showed characteristic bands at 1625 cm^{-1} which can be assigned as stretching vibration band of the azomethine group (-N=CH-). The bands in the ligand due to $\nu_{asymm}(SO_2)$ and $\nu_{symm}(SO_2)$ appeared at 1333 and 1163 cm^{-1}, respectively. A high intensity band at 1306 cm^{-1} can be assigned to the naphthalic (C–O) group and the band at 1072 cm^{-1} is assigned to the stretching vibration of N–N group of the free ligand. The OH band observed at 3048 cm^{-1} in the ligand spectrum disappeared in the IR spectrum of the complex. This indicates that the OH group was deprotonated. The shift of the stretching frequency of the C–O group observed at 1306 cm^{-1} the free ligand to a higher frequency (at 1322 cm^{-1}) with complex formation is also evidence that the ligand coordinated with the oxygen atom of the C-O group to the metal ion. In the complex spectrum, the ν(C=N) stretching band shifted to a lower wavelength (1616 cm^{-1}) according to that of the free ligand. This result indicated that the ligand coordinated to the Ni(II) ion through the nitrogen atom of the azomethine [1,24, 25].

3.4. Electronic spectra and magnetic behavior

The electronic spectrum of the ligand (Fig. 5a) in DMSO solution (10^{-4} M) shows a band at 353 nm, which corresponds to n→π^* transition of the carbonyl group. The $\pi\rightarrow\pi^*$ transitions observed at 320 as a band and 308 nm as a shoulder was assigned to the aromatic rings and azomethine moiety, respectively. In the electronic spectrum of the complex (Fig. 5b), $\pi\rightarrow\pi^*$ and n→π^* transitions were observed at higher wavelengths than those in the spectrum of ligand (323nm, 336nm and 380 nm). The new absorption band at 438 nm for the complex are due to metal-ligand charge transfer processes. The d-d transitions could not be observed in the square planar nickel complexes, probably because their intensities are quite low. Hence, Square-planar structure may be assigned to this complex [24, 26].

The magnetic moment of the complex (as BM) was measured at room temperature. The four-coordinate Ni(II) complex exhibited magnetic moments of 0 B.M. The [NiL_2] complex has diamagnetic character, and the diamagnetic nature of the complex suggests a square planar geometry for the Ni(II) complex [10, 24].

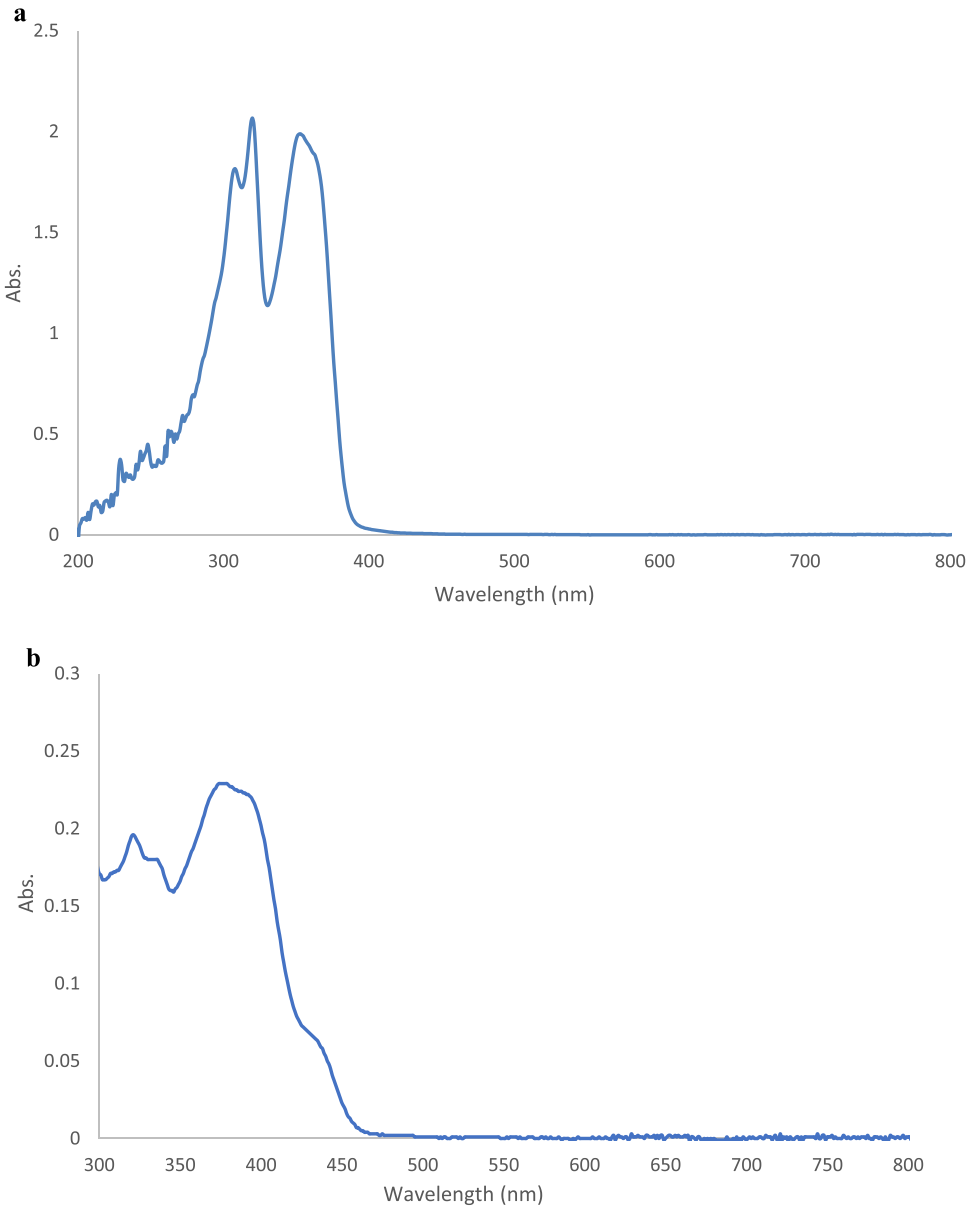

Fig. 5. a) Electronic spectrum of HL; b) Electronic spectrum of 1.

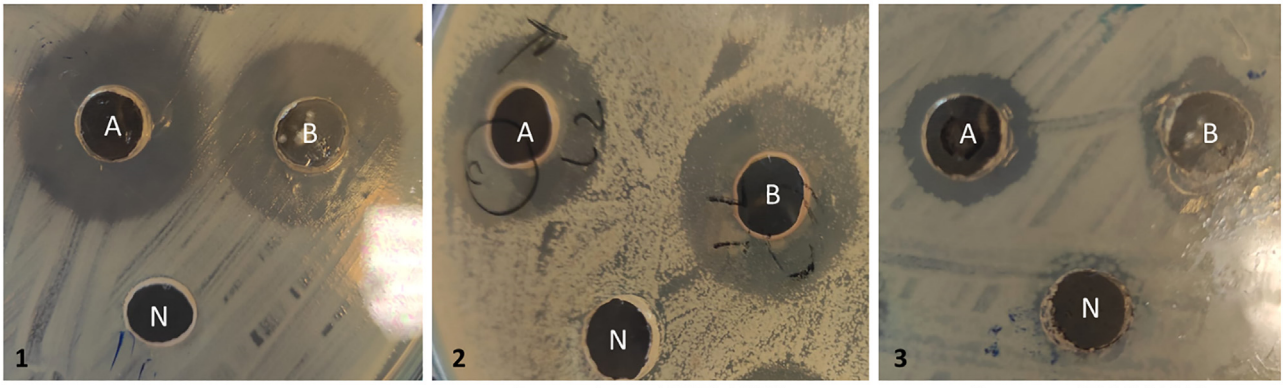

Fig. 6. Image of the antimicrobial zone diameters of nickel and its ligand on some pathogens. A: 1, B: HL, N: Control.

Table 4
Antimicrobial zone diameters of the nickel complex and its ligand.

Compounds	Antimicrobial zone diameter						
	E. coli ATCC 25922	P. aeruginosa ATCC 27853	S. aureus ATCC 29213	E. faecalis ATCC 29212	K. pneumoniae ATCC 13883	B. cereus CU1065	B. subtilus ATCC 6633
HL	17±0.36	17±0.56	13±0.36	12±0.54	-	14±0.85	16±0.45
1	18±0.28	17±1.23	14±0.24	15±0.38	-	16±1.01	17±0.37

3.5. Antimicrobial activity of HL and 1

The antimicrobial activity of the synthesized ligand and its Ni(II) complex on pathogenic microorganisms with high clinical importance was determined by the well diffusion method.

As shown in Table 4, both novel compounds showed antimicrobial activity in all strains except *K. pneumoniae* type strain. It was found that the inhibitory effects of the complex and the ligand were generally similar. It was determined that the complex and the ligand showed a strong inhibitory effect on *E. coli* and *P. aeruginosa*, which cause serious clinical infections, but had a weaker effect on *S. aureus*. (Fig. 6). On the *E. faecalis, B. cereus* and *B. subtilus* strains, it was determined that the complex showed more activity than the ligand.

4. Conclusions

In this study, new sulfonyl hydrazone ligand HL and its Ni(II) complex were synthesized. The structural characterizations of the synthesized compounds were made by using the elemental analysis, spectroscopic methods, and magnetic measurement. X-ray results showed that the HL crystallized in space group P 2_1/c. From the spectroscopic characterization and analytical data, it was concluded that the sulfonyl hydrazone ligand coordinated through imine nitrogen and phenolic oxygen to the metal ion. According to magnetic moment measurements, the [NiL_2] complex had square-planar geometry. The antibacterial activities of HL and its Ni(II) complex were assessed against clinically important human pathogens. It was determined that the inhibitory effects of HL and its Ni(II) complex were similar. While both compounds have no effect on the *K. pneumoniae* type, it has been determined that they have strong inhibitory effects on *E. coli* and *P. aeruginosa*, which cause serious clinical infections.

Declaration of Competing Interest

The authors declare that they have no known competing financial interests or personal relationships that could have appeared to influence the work reported in this paper.

Acknowledgments

This work was supported by the Ahi Evran University Scientific Research Projects Coordination Unit. (Project Number: AHİLAB.A4.22.001). The authors acknowledge the Central Research and Application Laboratory, Kırşehir Ahi Evran University. The authors acknowledge the Scientific and Technological Research Application and Research Center, Sinop University, Turkey, for the use of the Bruker D8 QUEST diffractometer. The authors gratefully acknowledge Dr. Esin Kıray (Kırşehir Ahi Evran University) and Prof. Dr. Çiğdem Yüksektepe Ataol (Çankırı Karatekin University).

References

[1] N. Özbek, Ü.Ö. Özdemir, A.F. Altun, E. Şahin, J. Mol. Struct. 1196 (2019) 707–719.
[2] M. Tahriri, M. Yousefi, K. Mehrani, M. Tabatabaee, D. Ashkezari, Pharmaceut. Chem. J. 51 (2017) 425–428.
[3] T. Tanaka, N. Yajima, T. Kiyoshi, Y. Miura, S. Iwama, Bioorg. Med. Chem. Lett. 27 (2017) 4118–4121.
[4] A.A.M. Abdel-Aziz, A. Angeli, A.S. El-Azab, M.E.A. Hammouda, M.A. El-Sherbeny, C.T. Supuran, Bioorg. Chem. 84 (2019) 260–268.
[5] N. Özbek, H. Katırcıoğlu, N. Karacan, T. Baykal, Bioorg. Med. Chem. 15 (2007) 5105–5109.
[6] A.C. Hangan, G. Borodi, R.L. Stan, E. Pall, M. Cenariu, L.S. Oprean, B. Sevastre, Inorg. Chim. Acta 482 (2018) 884–893.
[7] S. Alyar, C. Şen, H. Alyar, S. Adem, A. Kalkancı, Ü.Ö. Özdemir, J. Mol. Struct. 1171 (2018) 214–222.
[8] Boyd, A.E., 3rd Diabetes 37 (1988) 847e850.
[9] S. Murtaza, S. Shamim, N. Kousar, M.N. Tahir, M. Sirajuddin, U.A. Rana, J. Mol. Struct. 1107 (2016) 99–108.
[10] N. Özbek, S. Alyar, H. Alyar, E. Şahin, N. Karacan, J. Mol. Struct. 108 (2013) 123–132.
[11] M. Çınarlı, Ç. Yüksektepe Ataol, H. Bati, F. Güntepe, H. Öğütçü, O. Büyükgüngör, Inorganica Chimica Acta 484 (2019) 87–94.
[12] M. Çınarlı, E. Çınarlı, Ç. Yüksektepe Ataol, Ö. İdil, E. Kariptaş, J. Mol. Struct. 1196 (2019) 760–770.
[13] G.M. Sheldrick, Acta Cryst. A71 (2015) 3–8.
[14] L.J. Farrugia, J. Appl. Crystallogr. 45 (2012) 849–854.
[15] G.M. Sheldrick, Acta Cryst. C71 (2015) 3–8.
[16] L.J. Farrugia, J. Appl. Crystallogr. 45 (2012) 849–854.
[17] A. Zülfikaroğlu, Ç. Yüksektepe Ataol, Hydrazones: Uses And Reactions, Nova Science Publishers, Inc. New York, 2020 Chapter 2.
[18] A. Zülfikaroglu, Ç. Yüksektepe Ataol, E. Çelikoglu, U. Çelikoglu, Ö. Idil, J. Mol. Struct. 1199 (2020) 127012.
[19] I. Kılıç-Cıkla, S. Güveli, T. Bal-Demirci, M. Aygün, B. Ülküseven, M. Yavuz, Polyhedron 130 (2017) 1–12.
[20] W. Cao, Y. Liu, T. Zhang, J. Jia, Polyhedron 147 (2018) 62–68.
[21] B. Jeragh, M.S. Ali, A.A. El-Asmy, Spectrochim. Acta Part A 145 (2015) 295–301.
[22] S. Demir, S. Cakmak, N. Dege, H. Kutuk, M. Odabasoglu, R.A. Kepekci, J. Mol. Struct. 1100 (2015) 582–591.
[23] S. Demir, F. Tinmaz, N. Dege, İ.Ö. Ilhan, J. Mol. Struct. 1108 (2016) 637–648.
[24] A.L. Spek, Acta Crystallogr. D65 (2009) 148–155.
[25] Ü.Ö. Özmen, G. Olgun, Spectrochimica Acta Part A 70 (2008) 641–645.
[26] B. Murukan, K. Mohanan, Transit. Metal Chem. 31 (2006) 441–446.